JOURNAL OF MATERIALS SCIENCE **38** (2003) 2505–2510

A study of the strength of P/M 6061Al and composites during high strain rate superplastic deformation

X. J. LI, M. J. TAN
Nanyang Technological University, Singapore 639798, Republic of Singapore
E-mail: mmjtan@ntu.edu.sg

Metal Matrix Composites (MMCs) are potential candidate materials in the aerospace and automobile industries because of its attractive properties, in particular, their high specific properties, and Superplastic forming (SPF) is a good solution to the problems in the forming process of MMCs due to their low ductility resulting from the incorporation of reinforcement. High strain rate superplasticity (HSRS) is attractive for industrial applications because superplastic forming at high strain rates can reduce forming time greatly. The strength of P/M 6061 Al and 6061 Al/SiC_p (3 μm) composites during superplastic deformation at temperatures of 853 K–871 K and a high strain rate of 0.1 s^{-1} has been studied in this paper. Experimental results presented a softening effect by the SiC_p reinforcement. Mechanical and microstructural analyses show that the decrease in the strength during high strain rate superlastic (HSRS) deformation is associated with the decreased grain size of the Al matrix with increase of the SiC_p volume fraction or the extrusion ratio, and the occurrence of liquid phase. The formation of the liquid phase was related to segregation of the solute atom during HSRS deformation.

1. Introduction

High strain rate superplasticity (HSRS) was first observed in 1984 in Al based metal matrix composite (MMCs) by T. G. Nieh *et al*. [1]. HSRS is attractive for industrial applications because the strain rate of HSRS (typically higher than 0.01 s^{-1}) is much faster than that of conventional superplasticity (10^{-5}–10^{-3} s^{-1}) [2], and consequently, the high strain rate superplastic forming will lead to great reduction in forming time.

Normally, the SiC_p reinforcement has a strengthening effect for the P/M 6061 Al/SiC_p composites. Such strengthening effect is usually due to various factors, e.g., refinement of subgrain size [3], load transfer [4] or effective barriers to dislocation motion [5]. However, some experiments on MA 2024 Al/SiC_p composites [6] and MA 2124 Al/SiC_p composites [7] showed a softening effect caused by reinforcement during HSRS deformation. To study this interesting phenomenon is helpful to get a better understanding of the deformation mechanism of HSRS.

Taking into account the threshold stress, the stress-strain relationship during deformation in a superplastic material is described by a power-law empirical equation [8],

$$\dot{\varepsilon} = A\frac{DGb}{kT}\left(\frac{b}{d}\right)^p\left(\frac{\sigma-\sigma_0}{G}\right)^n \tag{1}$$

where $\dot{\varepsilon}$ is the strain rate, σ the flow stress, σ_0 the threshold stress, A the constant, D the diffusion coefficient, G the shear modulus, b the Burgers vector, k the Boltzman constant, T the absolute temperature, d the grain size, n the stress exponent, p the inverse grain size exponent (=2–3). Equation 1 could be rewritten as,

$$\sigma = K\dot{\varepsilon}^{1/n} + \sigma_0 \tag{2}$$

where

$$K = \left[\frac{kT}{ADb^{p+1}}G^{n-1}d^p\right]^{\frac{1}{n}} \tag{3}$$

Equation 2 gives the strength of the material during HSRS deformation. It is affected by many factors such as G, d, n and so on. The purpose of this paper is to analyze the strength of P/M 6061 Al and composites during HSRS deformation in terms of mechanics and microstructural observations.

2. Experimental procedures

The α-type silicon carbide powder with diameter of 3 μm was used as reinforcement in this study. The chemical composition (wt%) of the 6061 Al matrix powders is 0.95Mg, 0.64Si, 0.29Cu, 0.24Fe, 0.03Mn, 0.07Cr, 0.03Ti, 0.05Zn and Al balance. The materials tested were fabricated using a powder metallurgy process. The as-mixed powders were hot-pressed in an Instron 8501 hydraulic machine at a temperature of

TABLE I Codes of P/M 6061 Al and composites

Code	SiC_p volume fraction (%)	Extrusion ratio
Al6061	0	20
MMC1	10	20
MMC2	18	20
MMC3	10	47

773 K and a load of 130 MPa. The as-hot-pressed billet was subsequently hot-extruded at 773 K. The extrusion ratios were selected as 20 and 47.

The tensile specimens with gauge length of 5 mm and diameter of 2.5 mm and 2 mm were machined from the extrudates. Four materials with different SiC_p volume fractions and extrusion ratios were investigated in this work. The details for them are shown in Table I. Tensile tests were conducted at 853 K–871 K and a high strain rate of 0.1 s^{-1}.

3. Results and discussions

3.1. Strength during HSRS deformation

Fig. 1 shows true stress-true strain curves of Al6061 (unreinforced, 20 : 1), MMC1 (10 vol%SiC_p, 20 : 1), MMC2 (18 vol%SiC_p, 20 : 1) and MMC3 (10 vol%SiC_p, 47 : 1) after deformation at 853 K–871 K and 0.1 s^{-1}. Several observations can be made below.

(1). The strength of the test materials (as measured by the true stress) during HSRS decreases with increasing SiC_p volume fraction. This is in good accord with the previous work [6, 7]. On average, the difference in the strength between 6061Al (unreinforced, 20 : 1) and MMC1 (10 vol%SiC_p, 20:1), and also between MMC1 and MMC2 (18 vol%SiC_p, 20 : 1) is 6 MPa and 5 MPa respectively.

(2). By comparison of the strength of MMC1 (10 vol%SiC_p, 20 : 1) and MMC3 (10 vol%SiC_p, 47 : 1) during HSRS deformation, we can see that the extrusion ratio has a significant effect on the strength; the magnitude of the strength decrease is 10 MPa by increasing the extrusion ratio from 20 to 47 at current testing conditions.

(3). At the same extrusion ratio, i.e. 20, the true strain ($\varepsilon_t = \ln(1+\varepsilon)$, where ε_t is the true strain, ε is the elongation-to-failure.) increases as the SiC_p volume fraction is increased. It can also be seen that for the material containing the same SiC_p content, a higher extrusion ratio leads to larger elongation-to failure.

(4). For all the test materials, lower strength during HSRS deformation is associated with larger elongation-to-failure, implying that the lower the strength, the higher the ability of P/M 6061 Al/SiC_p composites to exhibit superplasticity at high strain rate, and hence fast forming times and HSRS.

The curves of stress vs strain are a reflection of many complex internal processes that represent an averaged effect of all the operating parameters. Thus, the preceding results suggest that the SiC_p volume fraction and the extrusion ratio have significant effects on HSRS.

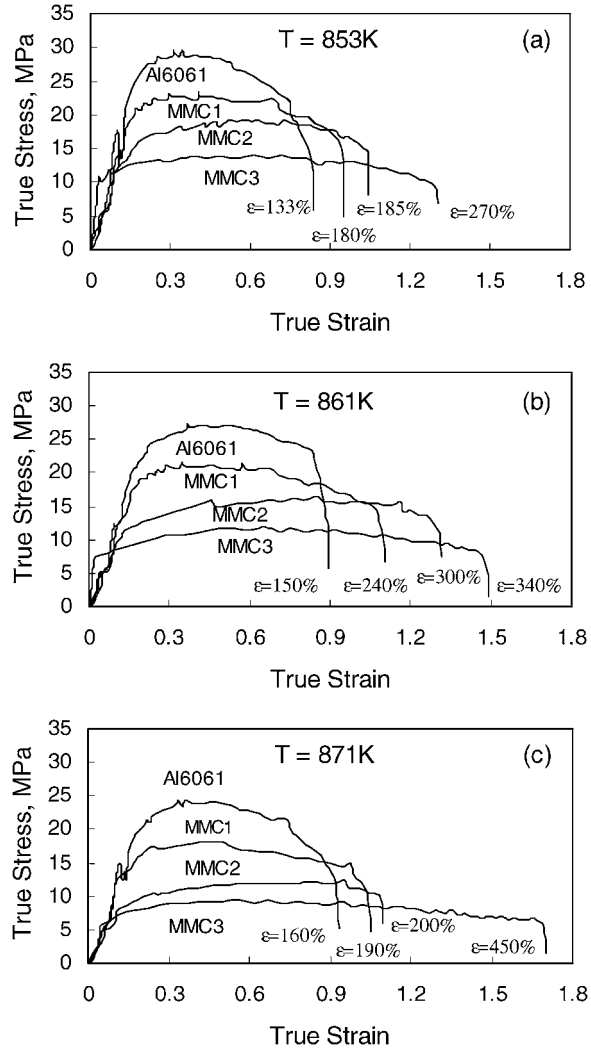

Figure 1 True stress-true strain curves of Al6061 (unreinforced, 20 : 1), MMC1 (10 vol%SiC_p, 20 : 1), MMC2 (18 vol%SiC_p, 20 : 1) and MMC3 (10 vol%SiC_p, 47) at 853 K–871 K and 0.1 s^{-1}. ε in this figure is the elongation-to-failure.

3.2. Factors affecting the strength during HSRS deformation

It is known from Equation 2 that the value of the strength (σ) at the same temperature and strain rate is dependent on three factors: K, n and σ_0. Using the best linear fit method, the experimental results in Fig. 1 obey Equation 2. The fitted results of the stress-strain rate relationship for Al6061, MMC1, MMC2 and MMC3 at 853 K–871 K at 0.1 s^{-1} are given in Table II.

3.2.1. Effects of SiC_p volume fraction on the strength during HSRS deformation

The Al6061, MMC1 and MMC2 specimens are selected to evaluate the Effects of SiC_p volume fraction on the strength during HSRS deformation. It can be found from the data in Table II that the slope of the fitted line (K) and the stress exponent (n) (from Equation 2) decrease the SiC_p volume fraction was increased. Obviously, the decrease in the K-value leads to the decrease in the σ-value. The difference in the values of their threshold stresses (σ_0) is less than 1.5 MPa. Thus, with increase in the SiC_p volume fraction, the decrease in the

TABLE II Stress-strain rate relationship for Al6061, MMC1, MMC2 and MMC3 at 853 K–871 K at 0.1 s^{-1}

Material	$T = 853$ K	$T = 861$ K	$T = 871$ K
Al6061	$\sigma = 39.44\dot{\varepsilon}^{1/4} + 3.59$	$\sigma = 36.85\dot{\varepsilon}^{1/4} + 2.46$	$\sigma = 30.92\dot{\varepsilon}^{1/4} + 2.54$
MMC1	$\sigma = 33.77\dot{\varepsilon}^{1/3} + 3.15$	$\sigma = 30.88\dot{\varepsilon}^{1/3} + 2.49$	$\sigma = 26.12\dot{\varepsilon}^{1/3} + 2.01$
MMC2	$\sigma = 29.38\dot{\varepsilon}^{1/3} + 1.72$	$\sigma = 27.41\dot{\varepsilon}^{1/3} + 1.00$	$\sigma = 21.93\dot{\varepsilon}^{1/3} + 0.64$
MMC3	$\sigma = 27.21\dot{\varepsilon}^{1/2.5} + 1.65$	$\sigma = 23.39\dot{\varepsilon}^{1/2.5} + 0.73$	$\sigma = 19.08\dot{\varepsilon}^{1/2.5} + 0.82$

σ-value for all the four materials mainly comes from the decrease in the K-value and the n-value, and are discussed below.

3.2.1.1. Decrease in K-value with increasing SiC_p volume fraction. Let $A_1 = \frac{kT}{ADb^{p+1}}$, then Equation 3 becomes

$$K = \left[A_1 G^{n-1} d^p\right]^{\frac{1}{n}} \tag{4}$$

where A_1 is a constant. This suggests that at a given temperature, the K-value is dependent on the shear modulus (G), the stress exponent (n) and the grain size of the matrix. Generally, the value of G increases with increasing reinforcement volume fraction. As can be seen in Equation 4, larger G-value leads to larger K-value. Hence, the decrease in the K-value with increase of SiC_p volume fraction is independent of the increase of the G-value.

To examine the influence of the stress exponent (n) on the K-value, differentiate both sides of Equation 4 with respect to n, then we have

$$\frac{\partial K}{\partial n} = \frac{K}{n}\left(\frac{n-1}{G} - \ln K\right) \tag{5}$$

A relationship between the shear modulus (G) and the absolute temperature (T) was expressed as $G = 4.4 \times 10^4 - 14\mathrm{T}$ (MPa) for the 6061 Al/SiC_w composite [9] and $G = 3.022 \times 10^4 - 16\mathrm{T}$ (MPa) for Al [10]. In this study, $T = 861$ K, $n = 3$–4, and $27 < K < 37$. Taking $G > 2 \times 10^4$ MPa, then $\frac{\partial K}{\partial n} < 0$. That is, the larger the n-value, the lower the K-value. From the experimental results and preceding discussion on the effects of the SiC_p volume fraction on the m-value for HSRS, it has been known that the n-value decreases from 4 to 3 as the SiC_p volume fraction is increased from 0 to 18% at the same extrusion ratio of 20. Therefore, like the shear modulus (G), n is not responsible for the decrease of the K-value with increase of the SiC_p volume fraction.

In superplasticity, the grain size exponent, p, is often equal to 2 or 3. We know from previous results that under the same processing condition, the higher the SiC_p volume fraction, the larger the grain size (d) of the 6061 Al matrix. Therefore, it can be concluded that with increasing SiC_p volume fraction, the decrease in the K-value is attributable to the finer grain size of the 6061 Al matrix.

3.2.1.2. Decrease in the n-value with increasing SiC_p volume fraction. The strain rate superplasticity parameter ($m = 1/n$) is an indication of the superplastic potential behaviour of a material. A higher m-value means a suppression in the development of necking and leads to larger elongation. On the other hand, in HSRS, a fine grain size of the matrix (about <3 μm) is a necessary but insufficient condition [11]. This suggests that a lower n-value (higher m-value) is associated with a finer matrix grain size. In the other words, with increasing SiC_p volume fraction, the decrease in the n-value is related to the decrease in the grain size of the Al matrix, as will be discussed in Section 3.3.

3.2.2. Effects of the extrusion ratio on the strength during HSRS deformation

In order to study the effects of the extrusion ratio on the strength during HSRS deformation, the data for MMC1 and MMC3 in Table II are compared. Compared to the 10 MPa decrease in the σ-value (see Fig. 1), the difference in the σ_0-value is very small when the extrusion ratio is increased from 20 to 47. Accordingly, it is assumed that the strength, σ, is mainly affected by the K-value and the n-value, rather than the threshold stress, σ_0. Thus, the preceding discussion about the effects of the SiC_p volume fraction on the strength during HSRS is applicable to the effects of the extrusion ratio because of the constant G-value, the decreased n-value (see Table II) and the decreased grain size of the Al matrix (as will be shown in Section 3.3) with increasing extrusion ratio; i.e., at the same temperature, with increasing extrusion ratio, the decrease in the strength during HSRS is related to the decrease in the grain size of the Al matrix.

3.3. Effects of the SiC_p volume fraction and the extrusion ratio on the grain size of the Al matrix

From the above discussions in terms of mechanics, we can see that the decrease in the strength (σ) with increase of the SiC_p volume fraction or the extrusion ratio is, in essence, attributable to the decrease in the grain size of the Al matrix. In fact, a previous study on 6061 Al/SiC_p Composites [12] showed a relationship between the subgrain size and the Zener-Hollomon parameter, Z,

$$D^{-m} = a + b \ln Z \tag{6}$$

where D is the subgrain size, and a, b, and m are constants. Zener-Hollomon parameter, Z, can be expressed as

$$Z = \dot{\varepsilon} \exp(\Delta H / GT) \tag{7}$$

where $\dot{\varepsilon}$ is the strain rate, ΔH the activation energy for deformation, G the universal gas constant and T the

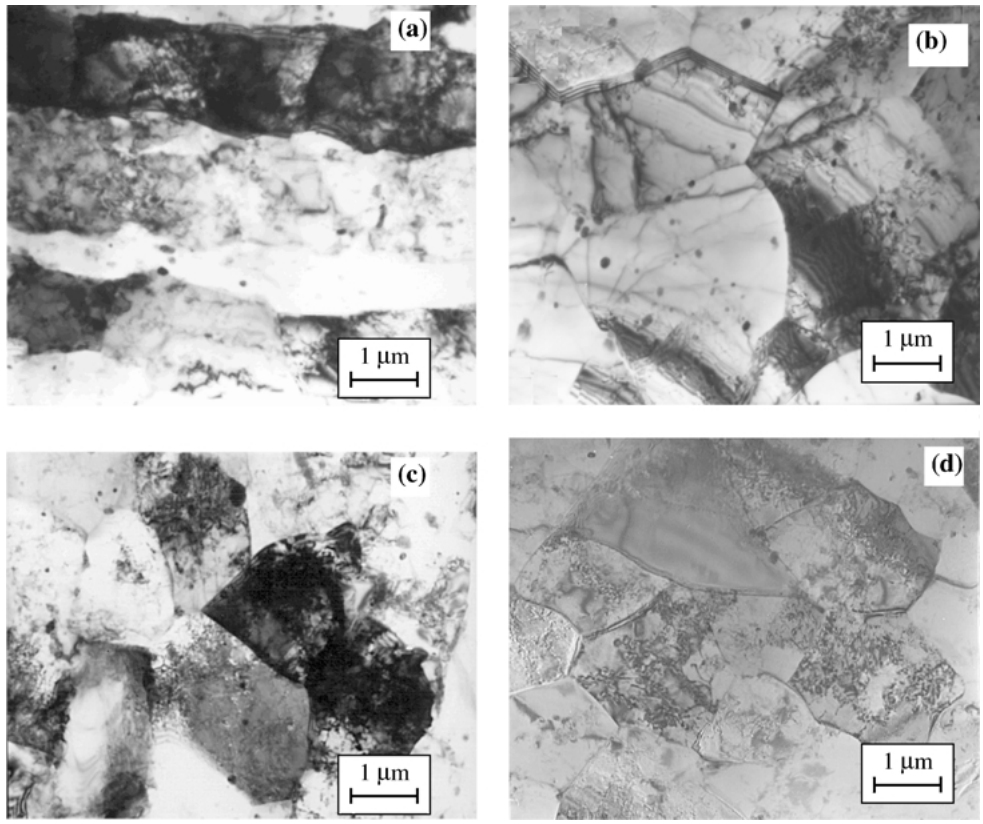

Figure 2 TEM microstructure of as-extruded specimens of 6061 Al and composites. (a).Al6061(unreinforced, 20); (b). MMC1 (10 vol%SiC_p, 20); (c). MMC2 (18 vol%SiC_p, 20); (d). MMC3 (10 vol%SiC_p, 47).

extrusion temperature in Kelvin. For the strain rate, $\dot{\varepsilon}$, a mean value can be calculated from Feltham's formula [13] in combination with the minimum-bound solution [14] as shown below,

$$\dot{\varepsilon} = \frac{6VD^2 \ln R \tan \varpi}{D^3 - d^3} \tag{8}$$

where V is the ram speed, R the reduction ratio, D and d the diameters of the billet and the extrudate respectively, and ω the semi-angle of the deformation zone given by

$$\varpi = 54.1 + 3.45 \ln R \tag{9}$$

where R is the reduction ratio. Obviously, the difference of the grain size obtained comes from the contribution of the reduction ratio, R. Because the reinforcement, SiC, is non-compressable, with increase in SiC_p volume fraction, the effective reduction ratio is increased during hot extrusion. Hence, according to Equation 7, as both the increase in the SiC_p volume fraction and in the extrusion ratio result in the decrease in the grain size of the Al matrix.

Fig. 2 shows the TEM microstructure of as-extruded specimens of the 6061 Al and composites. This is in agreement with above analyses. The aluminum matrix grains in the unreinforced 6061 Al alloy (Al6061, Fig. 2a) are heavily elongated. On the other hand, as a result of the incorporation of SiC particles and at certain hot-extrusion ratio, they become highly equiaxied (Fig. 2b and c). Increasing the SiC_p volume fraction or the extrusion ratio has the same effect on the microstructure of the 6061 Al matrix. The highly equiaxied and fine grain makes grain boundary sliding (GBS) easier than the heavily elongated grain.

3.4. Microstructure after fracture and liquid phase

The SEM morphologies of the fracture surface of the Al6061 (unreinforced, 20 : 1) and MMC3 (10 vol%SiC_p, 47 : 1) specimens in transverse direction tested at 871 K and 0.1 s^{-1} are shown Fig. 3a and b, where one can see that their fracture modes are quite different. The Al6061 specimen shows a typical ductile fracture with many dimples, while the MMC3 specimen is indicative of a viscous fracture surface with a large number of cavities arising from the extensive pull-out of SiC particles during deformation. Some viscous fiber-like boundaries in between two cavities (For instance, point "B" in Fig. 3b) is representative of the SiC_p/Al interface.

On the surface of the MMC3 specimen in Fig. 3d, extensive very fine filaments, which are often thought to be the evidence of liquid phase during high temperature deformation [15], were observed. Instead, very limited filaments on the surface of the Al6061 specimen in Fig. 3c. The observed viscous fracture surface (Fig. 3b) also supports the occurrence of liquid phase during HSRS deformation. The liquid phase could relax the stress concentration developed in the Al matrix near the triple junction and the reinforcement phase during high-temperature deformation. Its existence postpones the fracture of the material and leads to large elongation-to-failure. This can be exactly used to interpret why a maximum elongation-to-failure (450%) was

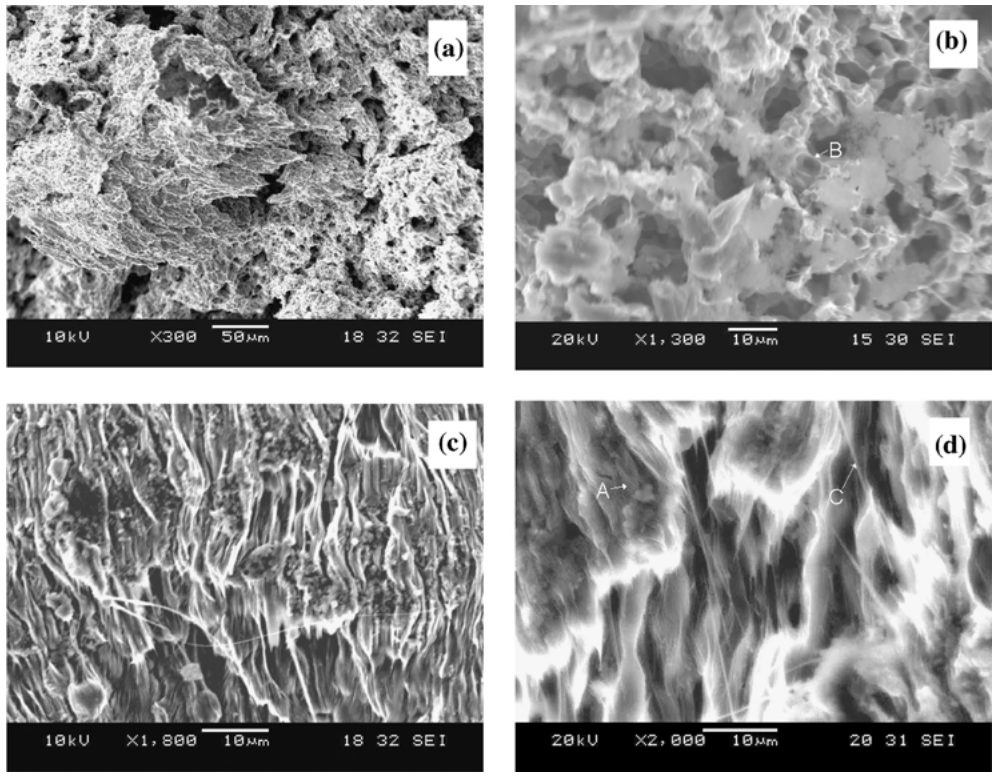

Figure 3 SEM microstructures of fracture surface of Al6061 (unreinforced, 20) and MMC3 (10 vol%SiC_p, 47) after deformation at 871 K and 0.1 s^{-1}. For (c) and (d), the longitudinal direction is vertical. EDS results of points A, B and C are presented in Fig. 4. (a). Al6061, transverse direction; (b). MMC3, transverse direction; (c). Al6061, longitudinal direction; (d). MMC3, longitudinal direction.

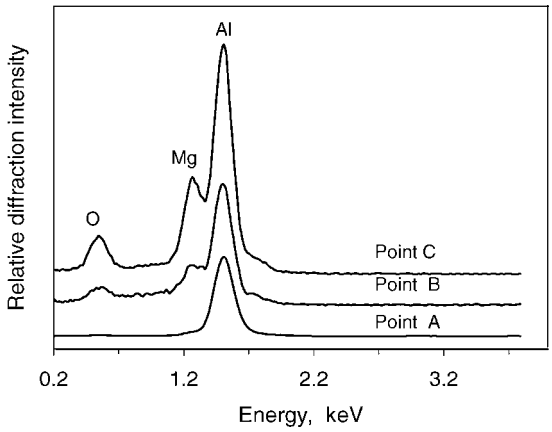

Figure 4 EDS results of points A, B and C of MMC3 after deformed at 871 K and 0.1 s^{-1}. The points are illustrated in Fig.3.

obtained in the MMC3 specimen at 871 K and 0.1 s^{-1} whereas the Al6061 specimen did not exhibit HSRS ($\leq$160%) under the same experimental conditions.

On the other hand, the existence of liquid phase decreases the strength of the material during HSRS deformation. The formation of liquid phase also explains softening effect by the SiC_p reinforcement observed during HSRS deformation.

In order to study the origin of the formation of liquid phase, EDS (Energy dispersive X-ray spectroscope) analysis was utilized to evaluate the chemical composition of the Al matrix and the filament. The EDS results were given in Fig. 4. The points A, B, and C detected in this figure are taken from Fig. 3. They represent the Al matrix, Al/SiC interface and the grain boundary with liquid phase (filament) respectively. As can be seen, Points B and C were composed of Al, Mg and O, while at Point A, only the matrix element Al was detected.

A previous study on the solute segregation to the Al alloys/SiC interfaces [16] revealed that the increase in Mg concentration due to the Mg segregation at grain boundaries and Al/SiC interfaces causes the decrease to some extent in the solidus temperature of 6061 Al alloy, leading to the formation of liquid phase. The enrichment of the oxygen in liquid phase is because the oxide film formed lacks necessary protection from further oxidation due to the low Pilling-Bedworth ratio of Mg [15].

A common experimental phenomenon about the formation of liquid phase is that it often occurs at grain boundaries and reinforcement/Al matrix interfaces. Therefore, the total areas of grain boundaries and reinforcement/Al matrix interfaces have noticeable effects on the amount of liquid phase formed. Finer grain size, finer particle size and more particles enhance the ability of the MMCs to exhibit HSRS. Returning to Figs 1 and 2, we can see that this is capable of accounting for the effects of the SiC_p volume fraction and the extrusion ratio on the strength and the elongation-to-failure in this study, that is, the more the SiC_p contents or the higher the extrusion ratio, the lower the strength (σ) during HSRS deformation and the larger the elongation-to-failure.

However, this is not appropriate to be used for explanation to the difference of the strength between the MMC2 (18 vol%SiC_p, 20 : 1) specimen and the MMC3 (10 vol%SiC_p, 47 : 1) specimen. As can be seen in Fig. 2, their Al matrix grain sizes are comparable. But it should be noted that the MMC2 specimen contains

more SiC particles. It appears that more liquid phase should be formed in the MMC2 specimen that in the MMC3 specimen, and the higher strength and lower elongation-to-failure should be obtained in MMC2 than in MMC3. However, the experimental data in Fig. 2 do not support this assumption. Thus, it can be assumed that the grain size of Al matrix plays a more important role in HSRS than the reinforcement content. A possible reason for this is that more serious strain, which enhances the segregation of solute atom (i.e. Mg in this study) to the grain boundary, is introduced because of higher extrusion ratio, as demonstrated in the EDS results in Fig. 4 that higher Mg concentration was detected at the grain boundary (Point A) than at Al/SiC_p interface (Point B).

It has been shown above that the softening effect by SiC_p reinforcement is strongly related to the grain size of the Al matrix both from the mechanical analysis and from the microstructural observations. This implies that there is a close relationship among the grain size of the matrix, liquid phase, the strength during deformation and the deformation mechanisms of HSRS. Work needs to be done to further study this relationship between the strain and the segregation of the solution atom.

4. Summary

P/M 6061 Al and composites with different SiC_p volume fraction were studied in this work. Tensile tests were conducted at 653 K–871 K and 0.1 s^{-1}. High Strain Rate Superplasticity (HSRS) is possible and the accompanying mechanisms are identified. The SiC_p reinforcement has a softening effect on P/M 6061 Al and composites during HSRS deformation. Mechanical analysis show that the decrease in the strength during HSRS deformation is associated with the fine grain size of the 6061 Al matrix.

From the microstructural aspect, the decrease in the strength is due to the occurrence of liquid phase. The formation of liquid phase results from the segregation of Mg at grain boundaries and SiC_p/Al matrix interfaces. The occurrence of liquid phase and composites reduces the strength of P/M 6061 Al and composites during HSRS deformation, and enhance their ability to achieve large elongation-to-failure. However, the grain size of the Al matrix appears to play a more important role in HSRS than the reinforcement content.

References

1. T. G. NIEH, C. A. HENSHALL and J. WADSWORTH, *Scripta Metall.* **18** (1984) 1405.
2. K. HIGASHI, T. OKADA, T. MUKAI and S. TANIMURA, *Mater. Sci. Eng.* **159A** (1992) 11.
3. V. C. NARDONE and J. R. STRIFE, *Metall. Trans.* **18A** (1987) 109.
4. G. GONZALEZ-DONCEL and O. D. SHERBY, *Acta Metall. Mater.* **41**(10) (1993) 2797.
5. R. S. MISHRA, T. R. BIELER and A. K. MUKHERJEE, *ibid.* **43**(3) (1995) 877.
6. K. MATSUKI, M. TOKIZAWA and S. MURAKAMI, *Materials Science Forum* **243–245** (1997) 309.
7. A. B. PANDEY, R. S. MISHRA and Y. R. MAHAJAN, *Acta Metall. Mater.* **40**(8) (1992) 2045.
8. B. Q. HAN and K. C. CHAN, *Scripta Materialia* **36**(5) (1997) 593.
9. F. A. MOHAMED and T. G. LANGDON, *Metall. Trans.* **5** (1974) 2339.
10. T. G. NIEH and J. WADSWORTH, *Materials Science and Engineering* **A147** (1991) 129.
11. M. MABUCHI, K. HIGASHI and T. G. LANGDON, *Acta Metall. Mater.* **42**(5) (1994) 1739.
12. X. XIA, P. SAKARIS and H. J. MCQUEEN, *Materials Science and Technology* **10** (1994) 487.
13. P. FELTHAM, *Metal Treatment* **23** (1956) 440.
14. J. F. ADIE and ALEXANDER, *Int. J. Mech. Sci.* **9**(6) (1967) 349.
15. C. L. CHEN and M. J. TAN, *Materials Science & Engineering* A **298**(1/2) (2000) 235.
16. M. STRANGWOOD, C. A. HIPPSLEY and J. J. LEWANDOWSKE, *Scr. Metall. Mater.* **24** (1990) 1483.

Received 5 December 2001
and accepted 9 August 2002